



# Glucose transporter 2 mediates the hypoglycemia-induced increase in cerebral blood flow

Hongxia Lei<sup>1,2</sup> , Frédéric Preitner<sup>3,4,\*</sup>, Gwenaël Labouèbe<sup>3,\*</sup>, Rolf Gruetter<sup>1,2,5</sup> and Bernard Thorens<sup>3</sup>

## Abstract

Glucose transporter 2 (*Glut2*)-positive cells are sparsely distributed in brain and play an important role in the stimulation of glucagon secretion in response to hypoglycemia. We aimed to determine if *Glut2*-positive cells can influence another response to hypoglycemia, i.e. increased cerebral blood flow (CBF). CBF of adult male mice devoid of *Glut2*, either globally (*ripglut1:glut2<sup>-/-</sup>*) or in the nervous system only (NG2KO), and their respective controls were studied under basal glycemia and insulin-induced hypoglycemia using quantitative perfusion magnetic resonance imaging at 9.4 T. The effect on CBF of optogenetic activation of hypoglycemia responsive *Glut2*-positive neurons of the paraventricular thalamic area was measured in mice expressing channelrhodopsin2 under the control of the *Glut2* promoter. We found that in both *ripglut1:glut2<sup>-/-</sup>* mice and NG2KO mice, CBF in basal conditions was higher than in their respective controls and not further activated by hypoglycemia, as measured in the hippocampus, hypothalamus and whole brain. Conversely, optogenetic activation of *Glut2*-positive cells in the paraventricular thalamic nucleus induced a local increase in CBF similar to that induced by hypoglycemia. Thus, *Glut2* expression in the nervous system is required for the control of CBF in response to changes in blood glucose concentrations.

## Keywords

Glut2, glut2 brain cells, cerebral blood flow, hypoglycemia, optogenetic

Received 30 October 2017; Revised 16 January 2018; Accepted 24 February 2018

## Introduction

A continuous supply of glucose from the systemic circulation to the brain is essential for sustained brain metabolism and function and any interruption of glucose delivery may lead to brain cell injury or death.<sup>1,2</sup> Hypoglycemia is a state of energy deficit incompatible with the maintenance of normal brain function and therefore elicits numerous hormonal responses to restore euglycemia, including an increased secretion of epinephrine and glucagon.<sup>3</sup> In addition, hypoglycemia also induces an immediate elevation of cerebral blood flow (CBF) in regions associated with increased autonomic response, a response consistently observed not only in humans but also in other mammals.<sup>1,4,5</sup> A local increase in CBF is also required for increased delivery of glucose in regions with augmented synaptic activity observed for instance during hypoglycemia and prevents hypoglycemia-associated cognitive impairments.<sup>5,6</sup> However, in diabetic patients, the normal

hypoglycemia-induced increase in blood flow becomes progressively impaired<sup>5,7,8</sup> in association with development of hypoglycemia associated autonomic failure.

<sup>1</sup>AIT, Center for Biomedical Imaging (CIBM-AIT), Ecole Polytechnique Fédérale de Lausanne, Lausanne, Switzerland

<sup>2</sup>Department of Radiology, University of Geneva, Geneva, Switzerland

<sup>3</sup>Center for Integrative Genomics, University of Lausanne, Lausanne, Switzerland

<sup>4</sup>Mouse Metabolic Evaluation Facility, Center for Integrative Genomics, University of Lausanne, Lausanne, Switzerland

<sup>5</sup>Department of Radiology, University of Lausanne, Lausanne, Switzerland

\*These authors contributed equally to this work.

## Corresponding authors:

Hongxia Lei, Center for Biomedical Imaging (CIBM), Ecole Polytechnique Fédérale de Lausanne, Lausanne CH-1015, Switzerland.

Email: hongxia.lei@epfl.ch

Bernard Thorens, Center for Integrative Genomics, University of Lausanne, Lausanne CH-1015, Switzerland.

Email: Bernard.Thorens@unil.ch

The mechanisms underlying the global increase of CBF upon hypoglycemia and how they become blunted in diabetes remain unclear. Experimental studies have suggested that the increased CBF upon insulin-induced acute hypoglycemia is comparable to the elevation of CBF at pharmacological doses of deoxyglucose.<sup>9</sup> Glucose responsive neurons activated by hypoglycemia, referred to as glucose inhibited (GI) neurons, have been characterized by electrophysiological recordings on acute brain slices and found to be present in several brain areas, in particular in the hypothalamus and brainstem.<sup>10–12</sup> Activation of GI neuron firing by hypoglycemia involves a decrease in glucose metabolism with the consequent activation of AMP-dependent protein kinase and closure of a chloride conductance, or of K<sup>+</sup> leak channels.<sup>13</sup> In preceding studies, we have shown that GI neurons from the nucleus tractus solitarius (NTS) expresses the glucose transporter *Glut2* and are involved in stimulating vagal nerve activity and glucagon secretion, linking hypoglycemia detection by the brain to the counterregulatory response.<sup>14</sup> More recently, we found that *Glut2* neurons in the paraventricular thalamic nucleus (PVT) are also activated by hypoglycemia. These are glutamatergic neurons that project to the nucleus accumbens and when activated by hypoglycemia, *Glut2* inactivation, or optogenetics they increase motivated sucrose seeking behavior in mice.<sup>15</sup> Immunohistological analysis of *Glut2* expression as well as genetic tagging of *Glut2*-expressing cells revealed that *Glut2* is expressed in relatively rare neurons, astrocytes and endothelial cells distributed in several brain areas.<sup>16–19</sup> As *Glut2* expression has been consistently associated with glucose sensing capacity,<sup>20</sup> this suggests that central *Glut2*-expressing cells may form a global glucose surveillance network. Here, we tested the hypothesis that brain *Glut2*-expressing cells control CBF in response to hypoglycemia.

In order to measure CBF, we used the arterial spin labeling (ASL) magnetic resonance imaging (MRI) technique, which provides a non-invasive measurement of the blood flow in the brain<sup>21,22</sup> that is superior to other exogenous contrast-agent based techniques, e.g. autoradiography,<sup>9,23</sup> positron emission tomography (PET<sup>24</sup>) and dynamic perfusion MRI.<sup>25</sup> Moreover, continuous ASL (CASL) using an actively-detuned two-coil system presents higher sensitivity and minimizes magnetization transfer effects and, thus, has been extensively used for brain studies in both rats<sup>21,22</sup> and mice.<sup>26,27</sup> Furthermore, the hypoglycemia-induced CBF increases measured in rats using the CASL technique<sup>28</sup> were similar to those obtained from ex vivo tissues using a diffusible indicator (i.e. 4-iodo-[N-methyl-<sup>14</sup>C] antipyrine).<sup>4,9</sup>

Thus, the aim of this study was to compare CBF under basal glycemia and upon insulin-induced

hypoglycemia in *Glut2*-null mice and their controls using the CASL MRI technique. We also used an optogenetic approach to test the impact on regional blood flow of selectively activating *Glut2*-positive GI neurons in the PVT.

## Methods

### Animals

All experiments were carried out with the approval of the Veterinary Office of Canton de Vaud and were conducted according to the Federal and Local ethical guidelines, EXPANIM (Expérience sur animaux-SCAV, Service de la consommation et des affaires vétérinaires, Switzerland) and in compliance with ARRIVE guidelines (Animal Research: Reporting in Vivo Experiments) for how to REPORT animal experiments. We used mice with systemic *Glut2* gene inactivation and transgenic expression of *Glut1* in pancreatic islet beta-cells to normalize glucose-stimulated insulin secretion (*ripglut1;glut2*<sup>-/-</sup> mice and their littermate controls: *ripglut1;glut2*<sup>+/-</sup>)<sup>29</sup> and mice with inactivation of the *Glut2* gene only in the central and peripheral nervous system *Glut2* (*glut2*<sup>Δ/loxP</sup>; *Nes*<sup>Cre/+</sup> (NG2KO) mice and their littermate controls: *glut2*<sup>Δ/lox</sup>; or *glut2*<sup>+/-lox</sup>; *Nes*<sup>Cre/+</sup>).<sup>30</sup> All mice studied had been backcrossed on the C57BL/6 background. For the optogenetic study, we used mice expressing channelrhodopsin2 in *Glut2*-positive cells (*glut2-cre; Rosa26ChR2-YFP*; mixed C57BL/6;SV129 background).<sup>14,15,18</sup>

For all experiments, adult male mice (10–15 weeks old) were used. Animals were collectively housed (maximum five individuals per cage) on a 12-h light/dark cycle (lights on at 7 a.m.) and fed with a standard chow (Diet 3436, Provimi Kliba AG).

### MR Experiments

For MR experiments, all mice were anesthetized in a chamber filled with 3% isoflurane mixed with air, which helped minimizing the effect of oxygen levels on CBF. Thereafter, the mice were placed in a home-built holder and fixed using one bite piece and two ear bars. Once mouse heads were secured, tail bleeds were sampled for blood glucose level measurements using a glucose meter (Bayer Breeze2, Bayer Inc.), which requires a 1 μL volume per test and delivers a sufficient glucose range for our study, i.e. 0.6–33.3 mmol/L. Through the entire studies, physiological conditions including respiration rate and rectal temperatures were monitored through an MR compatible monitoring system (SA Instruments, US) and maintained in the targeted range, i.e. 80–10 beats-per min and 36–37°C, by varying the percentage of isoflurane (i.e. 1–1.5%) and the

temperature of circulating warm water, respectively. Immediately at the end of the MR experiments, glycemia was measured again from tail bleeds and blood samples were withdrawn from some animals to ensure that pH was 7.3–7.5, PaCO<sub>2</sub> 35–45 mmHg and PaO<sub>2</sub> > 80 mmHg, in order to prevent their vascular effects on CBF.<sup>31</sup>

The MR experiments were performed in a horizontal 9.4T/26 cm magnet (Agilent Inc., US), with a 12-cm-diameter gradient (400 mT/m in 120  $\mu$ s) insert interfaced to a DirectDrive console (Vnmrj, Agilent Inc., USA). A <sup>1</sup>H quadrature coil consisting of two geometrically decoupled 12-mm-inner-diameter loops, resonating at 400 MHz, was used as a radio-frequency (RF) transceiver for MR imaging. An 8-mm-inner-diameter butterfly RF coil at 400 MHz was used for ASL. Both coils included PIN-diode-based active-detuning circuits, controlled by a CASL pulse sequence via a home-built switch board.<sup>26</sup>

### Neurochemical profile of hippocampus and hypothalamus

To assess potential effects of *glut2* gene inactivation on brain and its intracellular glyceamic state at basal glycemia, a localized <sup>1</sup>H MR spectroscopy sequence was applied to two brain regions, e.g. hippocampus (~4  $\mu$ L) and hypothalamus (~4  $\mu$ L<sup>16–19</sup>), of five *rip<sup>glut1</sup>; glut2<sup>-/-</sup>* mice and five control littermates under basal (random fed) glycemia, as previously described.<sup>32</sup> This allowed assessing abundant metabolites involved in neurotransmission and metabolism from defined brain volumes, including all cells, extracellular space, and bloodstream. Cerebrospinal fluid contributes minimally to the measured metabolites in bilateral hypothalamus and even less so in unilateral hippocampus.<sup>32</sup> Sufficient signal-to-noise ratios (SNRs > 15) were achieved by averaging 160–320 scans for <sup>1</sup>H MR spectra. The water signal (eight scans) was acquired from the identical volumes of interests for further quantification, as described below.

### CASL of CBF

The CASL pulse sequence was implemented with a semi-adiabatic Spin-Echo Echo Planer Imaging (SE-EPI) sequence with both negative and positive reference scans by including additional labeling components, i.e. a 2.1-s hard RF pulse, a z-gradient (14 mT/m) and 1 s delay.<sup>26</sup> Such SE-EPI images are more representative of capillary perfusion.<sup>33</sup> Each labeling plane was carefully selected based on serial anatomical neck images (gradient-echo, 0.4-mm slice thickness, 20  $\times$  20 mm<sup>2</sup>, RO  $\times$  PE = 128  $\times$  128, nt = 8). The resulting CBF values of cortex, hippocampus, thalamus and

hypothalamus can be obtained with minimal magnetization transfer residuals.<sup>26</sup>

Anatomical images of murine brains were acquired using a fast spin echo (FSE) sequence (TE<sub>effective</sub>/TR = 50/4000 ms, a 20 mm  $\times$  20 mm field of view (FOV), readout (RO)  $\times$  phase-encode (PE) = 256  $\times$  256, 8 averages). Both first- and second-order shim terms were automatically adjusted over the murine brain (a 6  $\times$  4  $\times$  5 mm<sup>3</sup> volume of interest, VOI) using an EPI version of FASTMAP.<sup>34</sup> A localized water signal was acquired from the volume covering the entire brain to examine the field homogeneity within the VOI. Immediately after improving field homogeneity, 16 pairs of four or eight-segmented semi-adiabatic SE-EPI images were acquired to map CBF (TE = 42 ms, FOV = 23  $\times$  15 mm<sup>2</sup>, RO  $\times$  PE = 128  $\times$  64, spectral width = 200 kHz, 1.5–2.0 mm slice thickness).<sup>26</sup> For CBF in response to hypoglycemia, the EPI image slices were carefully positioned by referencing to the dorsal edge of the ventral hippocampal commissure (vhc) at Bregma –0.8 mm to have two MR image slices centered at Bregma 1 mm and –2 mm, respectively. The total acquisition time was approximately 6 or 13 min.

### CBF measurements under resting glycemia and insulin-induced hypoglycemia

To evaluate CBF responses upon insulin-induced hypoglycemia, *rip<sup>glut1</sup>; glut2<sup>-/-</sup>* mice ( $n = 7$ ) and their wild type counterparts ( $n = 6$ ) were studied at basal glycemia and following insulin-induced hypoglycemia. Six NG2KO mice and six of their age-matched control littermates were similarly studied.

A cannula was placed in the femoral vein, and mice were placed in the holder for the CASL measurements and a first CBF determination in basal glyceamic conditions was performed over a 20-min period, as described above. Then, to induce hypoglycemia, the animals along with the entire fixation system, including the RF coils, were carefully removed from the magnet and placed securely outside the magnetic field. A 1 U/kg bolus of insulin (1 U/ml, Lilly Inc., US) was given in 20 min. Once the hypoglycemic condition was reached, i.e.  $\leq 2.5$  mmol/L, a minimal continuous rate of insulin (in the range of 2–4 mU/kg) was maintained, and animals were carefully placed back to the original position in the magnet. Right after relocating the original slice of interest based on both transverse and sagittal images, i.e. in a 0.01 mm precision with our existing MR system, field homogeneity was slightly adjusted. Then, CBF measurements were performed on the nearly matching slice (e.g. <1% error to a 0.01 mm shift) in the very same animals using the identical CASL parameters over a

20-min period. A typical experimental layout is shown in Supplementary Figure 1.

The validity of the present protocol to study central effects of hypoglycemia on CBF relies on the absence of potential alterations of CBF secondary to peripheral cardiovascular changes. Isoflurane anesthesia minimally affects heart rate and pressure in mice.<sup>35</sup> Likewise, hypoglycemia is unlikely to secondarily alter CBF in our experiments. Indeed, firstly, while hypoglycemia was shown to increase heart rate – but not blood pressure,<sup>6</sup> we observed in parallel bench experiments using the MouseOx<sup>®</sup> module (Starr Life Science Corp, USA) in three control mice undergoing an identical CBF protocol, that heart rate did not significantly change during the experiment, i.e. between the basal and hypoglycemic periods ( $p > 0.05$ ), or from beginning to end of the basal period ( $457 \pm 75$  bpm vs.  $482 \pm 46$  bpm (mean  $\pm$  SD) respectively,  $p > 0.05$ ) and hypoglycemic phase ( $495 \pm 39$  bpm and  $506 \pm 36$  bpm, respectively,  $p > 0.05$ ). Secondly, CBF is highly autoregulated so that it remains independent of peripheral blood flow within a wide range of physiological cardiovascular states,<sup>1,31</sup> and the observed heart rate ranges in our bench experiment were well within the physiological range for CBF autoregulation.<sup>35</sup> As CBF is altered by both hypercapnia and poor blood oxygenation,<sup>31</sup> appropriate PaCO<sub>2</sub> and PaO<sub>2</sub> values were maintained by controlling respiration rates in the range of 80–110 bpm by varying the delivery rate of isoflurane.<sup>26</sup>

### Optogenetics

Ten to fifteen weeks old *glut2<sup>Cre/+</sup>;rosa26ChR2<sup>loxP/+</sup>* (*glut2Cre;rosa26ChR2<sup>lox/+</sup>*) and *glut2<sup>+/+</sup>;rosa26ChR2<sup>loxP/+</sup>* controls (*rosa26ChR2<sup>lox/+</sup>*) were used for in vivo optogenetics experiments. One week before the experiment, the mice were placed in a stereotaxic frame (David Kopf Instruments, U.S.A) under isoflurane anesthesia. A custom made optical cannula made of a ceramic ferrule (Precision Fiber Products) and an optical fiber (0.39 NA, 200  $\mu$ m core diameter) was lowered in the PVT using the following stereotaxic coordinates: AP  $-0.4$ /ML  $+0.8$ /DV  $-3.4$  mm with a  $10^\circ$  angle to avoid any damage to the superior sagittal sinus. The optical cannula was secured on top of the skull with tissue adhesive (VetBond; 3M) and dental cement (Paladur; Heraeus-Kulzer). On the day of the experiment, the animals were prepared for CBF measurement, as described above. In addition, a DSPP laser (LRS-0473-GFM-00100-05; Laserglow Technologies) placed outside the MRI scanner room was connected to the mice via a fiber optic patch cable plugged to the fiber cannula. The light stimulation protocol consisted of the delivery of 473 nm

light pulses (10 ms light pulses at 20 Hz, 1 s on/1 s off, 15 mW) for 15 min during the acquisition of CBF measurements. CBF was monitored in anterior part of the PVT under basal and light-stimulated conditions. Basal CBF values were obtained by averaging CBF measurements before and after the optical stimulation.

### Data analysis

The acquired <sup>1</sup>H MR spectra were post-processed for quantification. Briefly, each spectrum was frequency-corrected, summed and prepared for further LCModel analysis. The water signal originating from the same VOIs without water suppression was assumed 80% for both hippocampal and hypothalamic tissues, as previously reported.<sup>32</sup> Data from mice with a basal (random fed) glycemia out of the 4–10 mM range were excluded in order to avoid any potential effect of mild hypoglycemia and acute hyperglycemia on the neurochemical profiles.<sup>36,37</sup>

CBF maps, in units of mL/100 g/min, were derived by pair-wise pixel-by-pixel calculation of label and control semi-adiabatic SE-EPI images as previously described<sup>26</sup>

$$\text{CBF} = \left[ \frac{\lambda}{T_1} \right] \times \left[ \frac{S_c - S_L}{S_L + (2\alpha - 1)S_c} \right] \quad (1)$$

where  $\lambda$  is the blood–brain partition coefficient for water (0.9),  $T_1$  is the brain tissue longitudinal relaxation time (1.9 s at 9.4 T),  $S_c$  is the control imaging signal intensity,  $S_L$  is the labeled image signal intensity, and  $\alpha$  is the labeling efficiency of ASL and assumed to be 0.8, as measured previously.<sup>26</sup> Regions of interests were manually drawn based on the acquired EPI images. For instance, two brain regions with abundant *Glut2* neurons, e.g. hippocampus and hypothalamus, and one low abundant *Glut2* region, cortex, were assessed. The whole brain was also evaluated. The percent changes of CBF were calculated based on the acquired CBF baselines under basal conditions, as above.

### Statistics

Data are shown as mean  $\pm$  SEM. Student *t*-test (paired/unpaired) was applied to single comparisons. In order to evaluate difference between genotypes or treatments, two-way ANOVA was used with two major factors, e.g. genotype and region for CBF, genotype and metabolite for neurochemical profiles, and genotype and treatments for CBF changes. Bonferroni post hoc tests were then applied. Differences were considered statistically significant when *p*-value was less than 0.05.



## Results

### Effects of systemic *Glut2* inactivation on neurochemical profiles of both hippocampus and hypothalamus

To evaluate the potential effects of *Glut2* inactivation on brain neurochemical profiles, including energy substrates, such as glucose, lactate, and other metabolites, we acquired  $^1\text{H}$  MR spectra in the hippocampus and hypothalamus of *ripglut1;glut2*<sup>-/-</sup> mice under basal (random fed) condition in five *ripglut1;glut2*<sup>-/-</sup> mice and five control littermates. MR spectra were obtained from both brain regions with excellent quality, and distinct regional differences in metabolite levels (Figure 1). The glycemia before and at the end of the measurements were  $9.3 \pm 0.6$  and  $7.3 \pm 2.0$  mM, respectively (paired *t*-test  $p = 0.34$ ) for control mice and  $6.1 \pm 0.2$  vs.  $5.0 \pm 0.2$  mM (paired *t*-test  $p < 0.03$ ) for *ripglut1;glut2*<sup>-/-</sup> mice. Despite these glycemic differences between control mice and *ripglut1;glut2*<sup>-/-</sup> mice, which are due to renal glucose excretion in the absence of *Glut2* from the proximal convoluted tubules, glucose levels in the hippocampus and hypothalamus were not different between strains ( $1.9 \pm 0.2$  vs.  $1.2 \pm 0.3$   $\mu\text{mol/g}$  in the hippocampus of control and mutant mice, respectively  $p = 0.093$ ;  $2.2 \pm 0.2$  vs.  $1.5 \pm 0.6$   $\mu\text{mol/g}$ , in the hypothalamus of control and mutant mice, respectively,  $p = 0.10$ ). This was also the

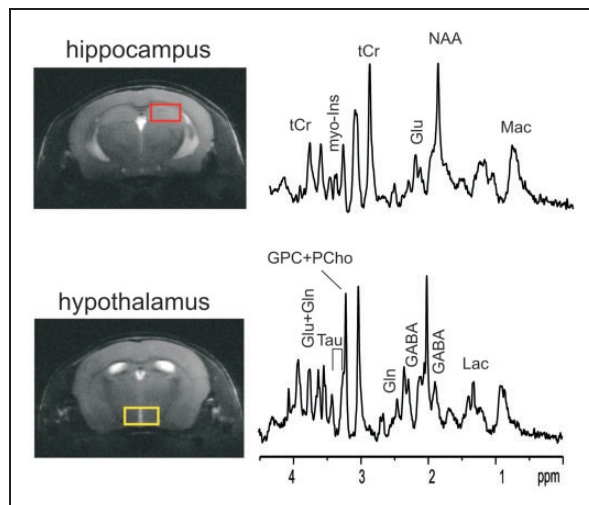


**Figure 1.** MR spectra of mouse brain hippocampus and hypothalamus. Localized MR spectra of hippocampus (red voxel in top MR image) and hypothalamus (yellow voxel in bottom MR image). Gln: glutamine; Glu: glutamate; tCr: total creatine; GABA:  $\gamma$ -aminobutyric acid; myo-Ins: myo-inositol; NAA: N-acetyl-aspartate; Mac: macromolecule; Lac: lactate.

case for all the other measured metabolites, except for a significant increase of myo-inositol in the hippocampus of *ripglut1;glut2*<sup>-/-</sup> mice (Figure 2).

### CBF of *ripglut1;glut2*<sup>-/-</sup> mice under resting/basal glycemia and insulin-induced hypoglycemia

For CASL-based measurement of CBF, another group of *ripglut1;glut2*<sup>-/-</sup> mice was studied. Multi-slice SE-EPI images were obtained with minimal artifacts or distortion and preserved anatomical structures, which allowed identifying regions of interest, e.g. hippocampus, hypothalamus, cortex and whole brain.

In basal conditions, CBF exhibited regional variations (Figure 3). A significantly higher CBF was observed in the hippocampus and hypothalamus of *ripglut1;glut2*<sup>-/-</sup> mice as compared to control mice (Figures 3(a) and 4(a) to (d)). When assessed in the cortex and the whole brain, no significant difference in CBF could be measured between strains. In control mice, blood glucose levels did not vary before and immediately after the CBF measurements ( $10.8 \pm 1.0$  mM vs.  $10.3 \pm 1.5$  mM, respectively; paired *t*-test  $p = 0.96$ ); in *ripglut1;glut2*<sup>-/-</sup> mice, glycemic levels tended to decrease ( $8.4 \pm 2.1$  mM vs.  $5.7 \pm 1.6$  mM, respectively; paired *t*-test  $p = 0.19$ ).

Next we determined CBF during insulin-induced hypoglycemia in *ripglut1;glut2*<sup>-/-</sup> mice ( $n = 7$ ) and their controls ( $n = 6$ ). In control mice, hypoglycemia ( $1.5 \pm 0.1$  mM, Figure 4(e)) significantly elevated CBF (Figures 3 and 4(a) to (d) and (f)) by  $28 \pm 10\%$  in hippocampus,  $38 \pm 10\%$  in hypothalamus,  $33 \pm 6\%$  in cortex and  $21 \pm 6\%$  in whole brain. In *ripglut1;glut2*<sup>-/-</sup> mice, hypoglycemia ( $1.0 \pm 0.1$  mM, Figure 4(e) and (f)) did not increase CBF except in the cortex where a small increase ( $5 \pm 3\%$ ) could be measured.

### CBF of NG2KO mice under resting/basal glycemia and acute hypoglycemia

To exclude potential contribution from peripheral *Glut2* and specifically assess the role of nervous system *Glut2* on CBF, we studied another mouse model, the NG2KO mice<sup>30</sup> in the basal state and upon insulin-induced hypoglycemia (Figure 3(b)), as described above.

In basal conditions, NG2KO mice and their controls (six of each) had similar glycemic levels, i.e.  $6.9 \pm 0.6$  mM vs.  $9.2 \pm 1.7$  mM (unpaired *t*-test  $p = 0.30$ ). NG2KO mice displayed significantly higher CBF than controls in the hypothalamus and the whole brain, but not in the hippocampus and cortex (Figure 5(a) to (d)).

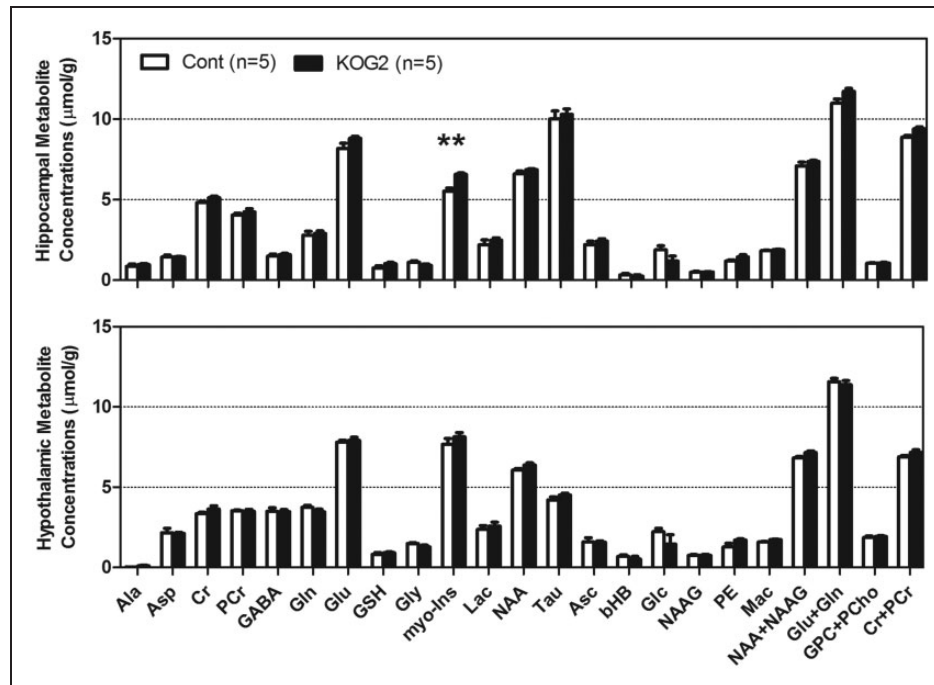


**Figure 2.** Neurochemical profiles of hippocampus and hypothalamus. Neurochemical profiles of hippocampus (Top) and hypothalamus (Bottom) of *rip glut1; glut2*<sup>-/-</sup> mice (KOG2, solid black bars,  $n=5$ ) and their age-matched controls (Cont, in white bars,  $n=5$ ) recorded in the basal state, revealed very minimal changes in *rip glut1; glut2*<sup>-/-</sup> (KOG2) mice except a small increase of myo-inositol (myo-Ins, arrow) in hippocampus (genotype:  $F(1,192) = 20.72$ ,  $p$ -value  $< 0.0001$ , metabolite:  $F(23,192) = 957.4$ ,  $p$ -value  $< 0.0001$ , interaction,  $F(23,192) = 2.209$ ,  $p$ -value = 0.002, Two-way ANOVA followed by the Bonferroni post-tests  $p$ -value  $< 0.01$ ). Ala: alanine; Asc: ascorbate; Asp: aspartate; bHB: beta-hydroxybutyrate; Cr: creatine; myo-Ins: myo-inositol; GABA:  $\gamma$ -aminobutyric acid; Glc: glucose; Gln: Glutamine; Glu: glutamate; Gly: glycine; GPC: glycerophosphocholine; GSH: glutathione; Lac: lactate; Mac: macromolecule; NAA: N-acetyl-aspartate; NAAG: N-acetyl-aspartyl-glutamate; PCho: phosphocholine; PCr: phosphocreatine; PE: phosphatidylethanolamines; Tau: taurine. NAA+NAAG, Glu+Gln, GPC+PCho, Cr+PCr and myo-Ins+Tau were included for statistical analysis but not displayed here. Error bars were SEMs.

Upon insulin-induced hypoglycemia (Figure 5(e)), control mice displayed increased CBF over all regions analyzed, e.g.  $14 \pm 3\%$  in hippocampus,  $24 \pm 4\%$  in hypothalamus,  $18 \pm 5\%$  in cortex and  $15 \pm 3\%$  in brain (Figure 5(a) to (d) and (f)). In contrast, hypoglycemia in NG2KO mice (Figure 5(e)), failed to increase CBF in the hippocampus ( $-2 \pm 4\%$ ), in the hypothalamus ( $-7 \pm 3\%$ ) and in the entire brain ( $-5 \pm 2\%$ ), with, however, a small increase in the cortex ( $11 \pm 7\%$ ) (Figure 5(a) to (d) and (f)). The higher CBF measured in both the *rip glut1; glut2*<sup>-/-</sup> mice and NG2KO mice in the basal state as compared to their respective controls suggests that inactivation of *Glut2*, by preventing glucose uptake, leads to an intracellular state of hypoglycemia sufficient to maximally activate the *Glut2* cells involved in CBF control.

#### Optogenetic activation of PVT *Glut2* neurons increases CBF

To directly evaluate the role of *Glut2*-expressing cells in the regulation of CBF, we determined whether optogenetic activation of *Glut2*-neurons of the PVT could

elicit a local increase in CBF. We previously reported that these PVT *Glut2* neurons form a homogenous population of glucose-inhibited neurons that control motivated sucrose seeking behavior.<sup>15</sup> Here, we equipped *glut2Cre; rosa26ChR2*<sup>lox/+</sup> mice and littermates not expressing channelrhodopsin with a fiber-optic cannula in the PVT. CASL measurements were performed in the basal state and during optical stimulation. Light stimulation of channelrhodopsin-expressing *Glut2*-neurons increased local CBF in the PVT by  $28 \pm 4\%$  (Figure 6); no such increase was observed in control ( $1 \pm 3\%$ , Figure 6). No differences in glycemia were found between the two groups, e.g.  $8.8 \pm 0.6$  mM in *glut2Cre; rosa26ChR2*<sup>lox/+</sup> mice and  $9.6 \pm 0.8$  mM in controls (unpaired  $t$ -test  $p=0.53$ ) before CBF measurements, and  $6.3 \pm 0.6$  vs.  $8.3 \pm 1.8$  mM (unpaired  $t$ -test  $p=0.33$ ) at the end of the measurements.

#### Discussion

The present study shows that systemic inactivation of *Glut2* or its inactivation only in the nervous system

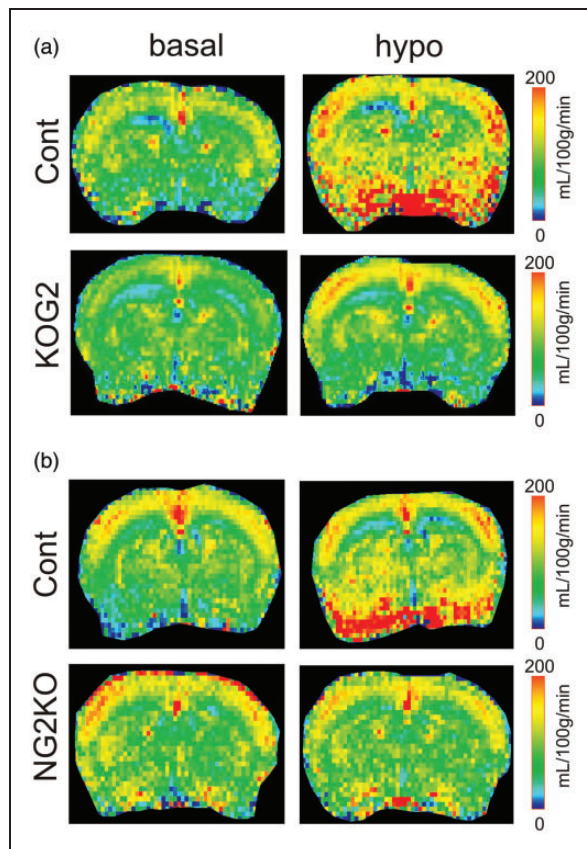


**Figure 3.** Cerebral blood flow color maps. Typical CBF maps of *ripglut1;glut2*<sup>-/-</sup> mice (KOG2 in a) and NG2KO mice (b) mice and their corresponding control littermates in basal conditions (*basal*, left column) and during insulin-induced hypoglycemia (*hypo*, right column). The typical CBF maps (mL/100 g/min) at Bregma 1 mm were scaled in the range of 0–200 mL/100 g/min to colors (see side bars).

increases CBF in basal glycaemic conditions but prevents its increase in response to insulin-induced hypoglycemia. This was observed in the whole brain and specifically in the hypothalamus and hippocampus, and to a lesser extent in the cortex. In addition, optogenetic activation of *Glut2*-neurons of the PVT was sufficient to increase local CBF. This study, thus, identifies *Glut2* expression in brain cells as a critical determinant of CBF response to hypoglycemia.

Previous immunohistochemical studies reported that *Glut2* is expressed in many brain regions where it is expressed by sparsely distributed neurons, glial or endothelial cells.<sup>16,17</sup> Mice expressing a fluorescent reporter protein under the control of the *Glut2* locus show a similar distribution of *Glut2*-expressing cells.<sup>18</sup> These central *Glut2* expressing cells were found to be required for glucose sensing and the control of various aspects of glucose homeostasis and feeding behavior.<sup>19,20,38</sup> In particular, we showed that central *Glut2*-dependent glucose sensing cells are required for the

control of glucagon secretion in response to hypoglycemia.<sup>18,19,39</sup>

In the present study, we extended these studies to assess the role of *Glut2* expressing cells in the CBF response to hypoglycemia using the non-invasive MR techniques. Absence of *Glut2* expression in *ripglut1;glut2*<sup>-/-</sup> mice had no effect on brain metabolites levels, impacting only slightly myo-inositol in the hippocampus but not in the hypothalamus. Notably, glucose levels in these two brain regions of *Glut2*-null mice were in the 1–2  $\mu\text{mol/g}$  range at euglycemia, in agreement with the fact that glucose transport through brain capillaries, a process that depends largely on *Glut1* expression in endothelial cells, represents the rate-limiting step for establishing parenchymal glucose levels.<sup>40</sup> In basal conditions, CBF was slightly, but significantly elevated in the hypothalamus of *ripglut1;glut2*<sup>-/-</sup> and NG2KO mice and in the hippocampus of *ripglut1;glut2*<sup>-/-</sup> mice when compared to their respective control littermates. Such increases in blood flow could not be explained by hypercapnia<sup>31</sup> or poor blood oxygenation since throughout the entire studies we maintained their respiration rates in the range of 80–110 bpm by varying the delivery rates of isoflurane that ensured appropriate PaCO<sub>2</sub> and PaO<sub>2</sub> values. Moreover, these CBF increases were seen despite the fact that we used isoflurane, an anesthetic vasodilator,<sup>41–43</sup> which can raise all measured blood flow values and thus might narrow the CBF differences between strains. Since we excluded animals with moderate acute hyperglycemia, which occurred occasionally in controls but less so in *ripglut1;glut2*<sup>-/-</sup> mice, plausible CBF variations<sup>44–47</sup> were ruled out from these CBF differences between strains.

Upon hypoglycemia, control mice displayed a marked increase in CBF in the cortex, the hippocampus and the hypothalamus, where the highest increase was observed. The increase in CBF induced by hypoglycemia was slightly lower in the NG2KO control group as compared to the *ripglut1;glut2*<sup>-/-</sup> control group; this may be attributed to slightly higher hypoglycemic levels of NG2KO controls compared to the *ripglut1;glut2*<sup>-/-</sup> control group (~1.8 mM vs. 1.5 mM, unpaired *t*-test *p*=0.09), similar to observations in rats.<sup>9</sup> It is striking that the absence of *Glut2* expression in both mouse models studied led to the same increase in CBF in the basal state and the absence of response during insulin-induced hypoglycemia, except for a small increase in the cortex. The brain as a whole showed a markedly blunted CBF response in both mouse models. The lower suppression of CBF in the cortex is consistent with a lower vulnerability to hypoglycemia of the cortical tissue compared to other brain regions<sup>1,48–50</sup> suggesting that whereas *Glut2*-dependent sensing is critical for adjusting CBF in many brain

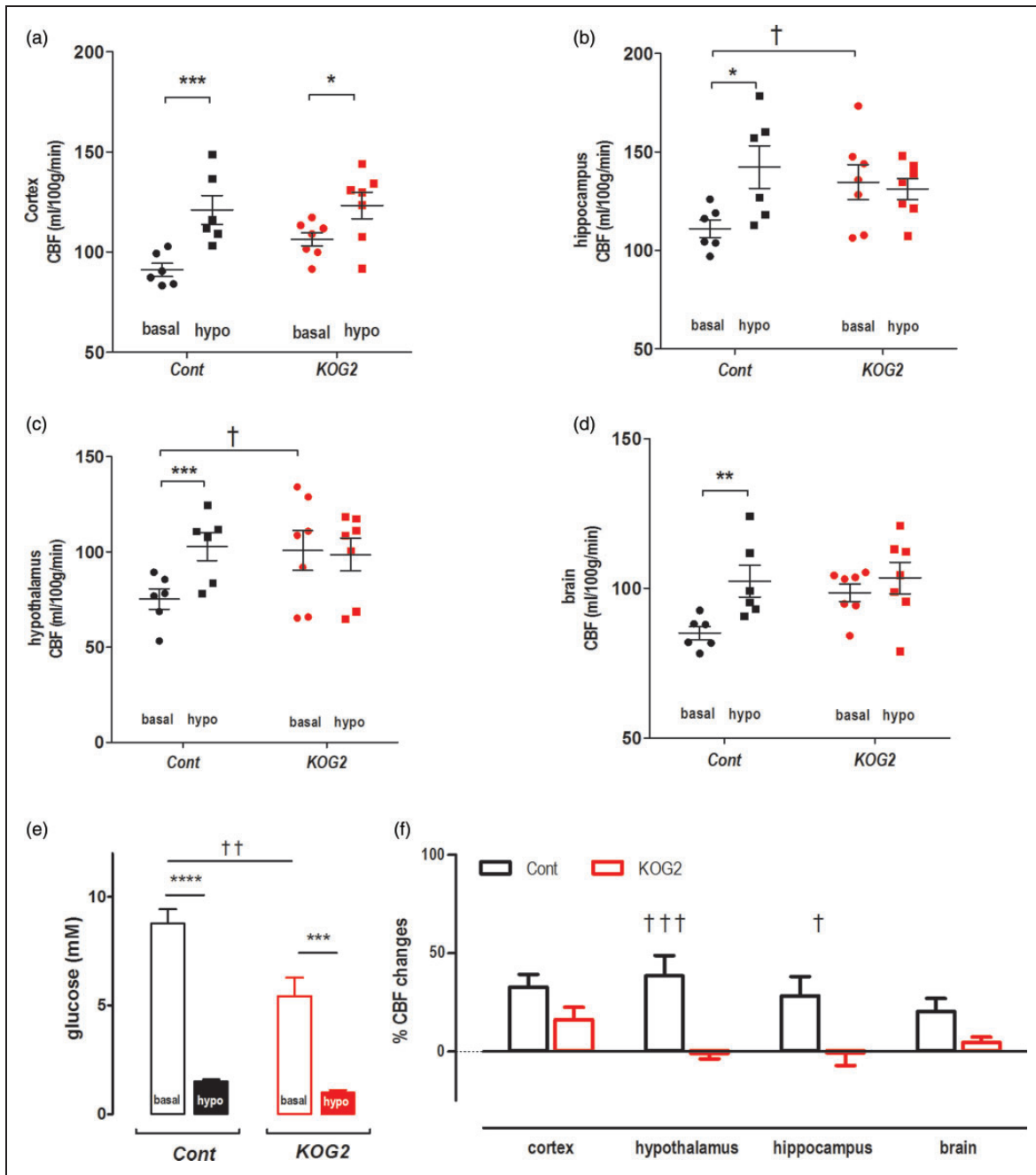


**Figure 4.** Impaired activation of CBF in *ripglut1; glut2<sup>-/-</sup>* mice during insulin-induced hypoglycemia. The CBF values (ml/100 g/min) of *ripglut1; glut2<sup>-/-</sup>* (KOG2) mice and their control littermates (Cont) were measured under basal glycaemic condition and insulin-induced hypoglycemia in different brain regions: (a) cortex, (b) hypothalamus, (c) hippocampus and (d) whole brain. (e) Glycaemic levels of control and *ripglut1; glut2<sup>-/-</sup>* mice under basal glycaemic condition and upon insulin-induced hypoglycemia. (f) Changes in CBF in the indicated brain regions of control and *ripglut1; glut2<sup>-/-</sup>* mice under insulin-induced hypoglycemia, expressed as percent of basal CBF values. Error bars were SEMs. Statistical significance: \* $p < 0.05$ , \*\* $p < 0.01$ , \*\*\* $p < 0.001$ , comparing treatments (two-way RM ANOVA with the Bonferroni post-tests), e.g. *basal* and *hypo*, in the same genotype groups. † $p < 0.05$ , †† $p < 0.01$ , ††† $p < 0.001$ , comparing genotypes, e.g. KOG2 vs. Cont, under the same glycaemic conditions (genotype and region factors, two-way ANOVA with the Bonferroni post-tests). When compare *basal* vs. *hypo* in the same genotype groups (a–d), two-way RM ANOVA was applied. Cont. treatment:  $F(1,20) = 52.73$ ,  $p$ -value  $< 0.0001$ , regions:  $F(3,20) = 10.81$ ,  $p$ -value  $= 0.0002$ , interaction:  $F(3,20) = 0.7462$ ,  $p$ -value  $= 0.5372$ ; K2GO. treatment:  $F(1,24) = 1.799$ ,  $p$ -value  $= 0.1924$ , regions:  $F(3,24) = 6.181$ ,  $p$ -value  $= 0.0029$ , interaction:  $F(3,24) = 2.4$ ,  $p$ -value  $= 0.0927$ . To compare genotype (a–d), two-way ANOVA was applied with *genotype and region factors* at *basal* and *hypo* conditions. *Basal*: genotype,  $F(1,44) = 20.01$ ,  $p$ -value  $< 0.0001$ ; region, ( $F(3,44) = 13.04$ ,  $p$ -value  $< 0.0001$ ); and interaction,  $F(3,44) = 0.4813$ ,  $p$ -value  $= 0.6970$ ; *hypo*: genotype,  $F(1,44) = 0.3470$ ,  $p$ -value  $= 0.5588$ ; region,  $F(3,44) = 11.12$ ,  $p$ -value  $< 0.0001$ ; interaction,  $F(3,44) = 0.3573$ ,  $p$ -value  $= 0.7841$ . In F, genotype:  $F(1, 44) = 28.71$ ,  $p$ -value  $< 0.0001$ , region:  $F(3, 44) = 1.319$ ,  $p$ -value  $= 0.2804$ , interaction:  $F(3, 44) = 1.408$ ,  $p$ -value  $= 0.2531$ .



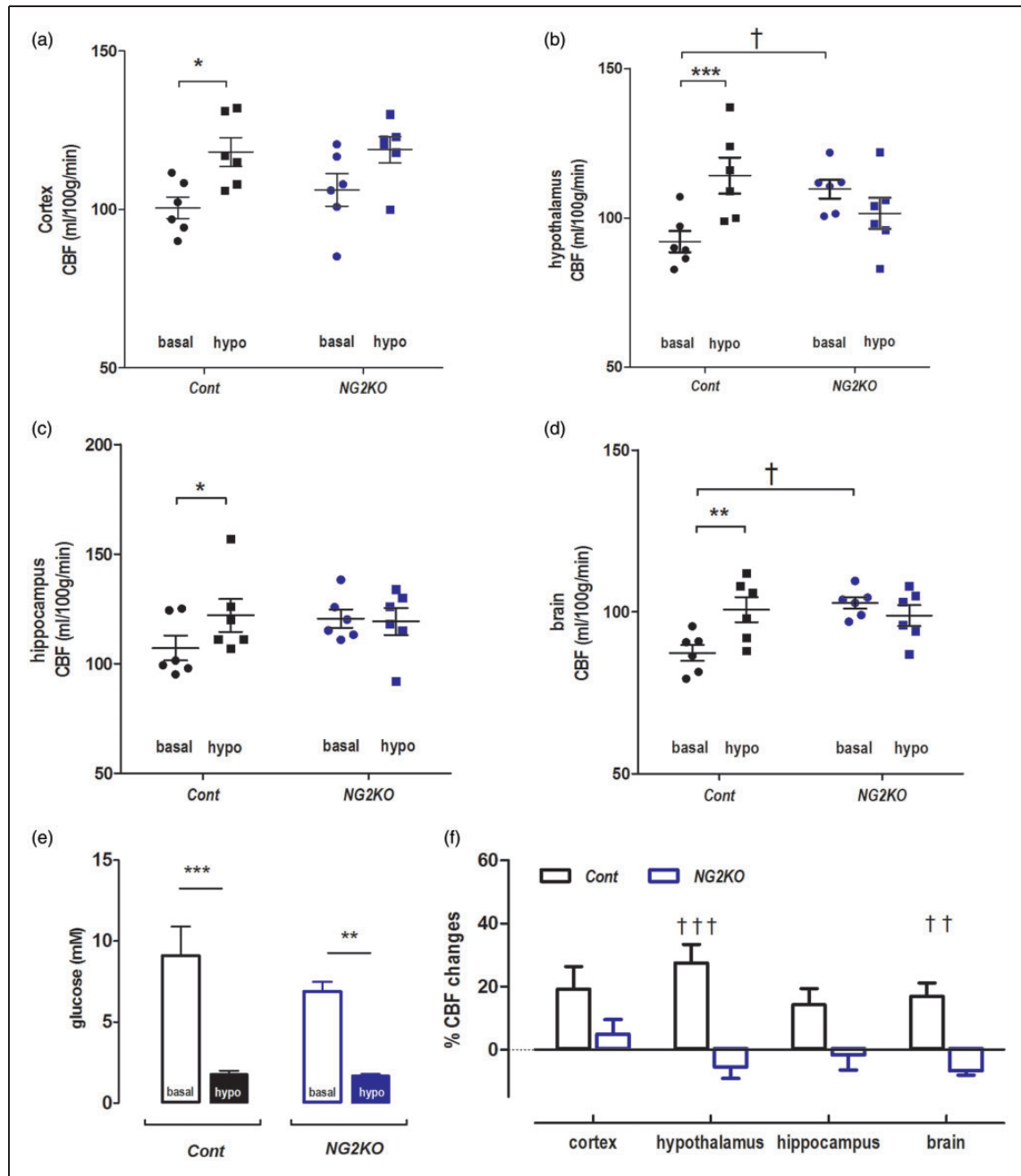


**Figure 5.** Impaired activation of CBF in NG2KO mice during insulin-induced hypoglycemia. The CBF values (ml/100 g/min) of NG2KO mice ( $n = 6$ ) and their control littermates (Cont,  $n = 6$ ) were measured under basal glycaemic condition and insulin-induced hypoglycemia in different brain regions: (a) cortex, (b) hypothalamus, (c) hippocampus and (d) whole brain. (e) Glycaemic levels of control and NG2KO mice under basal glycaemic condition and upon insulin-induced hypoglycemia. (f) Changes in CBF in the indicated brain regions of control and NG2KO mice under insulin-induced hypoglycemia, expressed as percent of basal CBF values. Error bars were SEMs. Statistical significance: \* $p < 0.05$ , \*\* $p < 0.01$ , \*\*\* $p < 0.001$ , comparing treatments (two-way RM ANOVA with the Bonferroni post-tests), e.g. *basal* and *hypo*, in the same genotype groups. † $p < 0.05$ , †† $p < 0.01$ , ††† $p < 0.001$ , comparing genotypes, e.g. NG2KO vs. Cont, under the same glycaemic conditions (genotype and region factors, two-way ANOVA with the Bonferroni post-tests). To compare *basal* vs. *hypo* in the same genotype groups (a–d), two-way RM ANOVA was applied (*treatment and region*). Cont: treatment,  $F(1,20) = 79.34$ ,  $p$ -value  $< 0.0001$ ; regions,  $F(3,20) = 3.862$ ,  $p$ -value  $= 0.0249$ ; interaction,  $F(3,20) = 1.028$ ,  $p$ -value  $= 0.4013$ ; Subjects (matching)  $p$ -value  $= 0.0002$ ; NG2KO: treatment,  $F(1,20) = 0.007026$ ,  $p$ -value  $= 0.934$ ; regions,  $F(3,20) = 4.919$ ,  $p$ -value  $= 0.0102$ ; interaction,  $F(3,20) = 4.274$ ,  $p$ -value  $= 0.0174$ ; Subjects (matching),  $p$ -value  $= 0.0098$ . To compare genotype (a–d), two-way ANOVA was applied with *genotype and region factors* at *basal* and *hypo* conditions. *Basal*: genotype,  $F(1,40) = 22.61$ ,  $p$ -value  $< 0.0001$ ; region, ( $F(3,40) = 8.249$ ,  $p$ -value  $= 0.0002$ ; and interaction,  $F(3,40) = 0.9113$ ,  $p$ -value  $= 0.4442$ ; *hypo*: genotype,  $F(1,40) = 1.252$ ,  $p$ -value  $= 0.2698$ ; region,  $F(3,40) = 6.802$ ,  $p$ -value  $= 0.0008$ ; interaction,  $F(3,40) = 0.6181$ ,  $p$ -value  $= 0.6074$ . In F (genotype and region factors), genotype:  $F(1,40) = 36.43$ ,  $p$ -value  $< 0.0001$ , interaction:  $F(3,40) = 2.811$ ,  $p$ -value  $= 0.0516$ , region:  $F(3,40) = 1.940$ ,  $p$ -value  $= 0.1387$ .

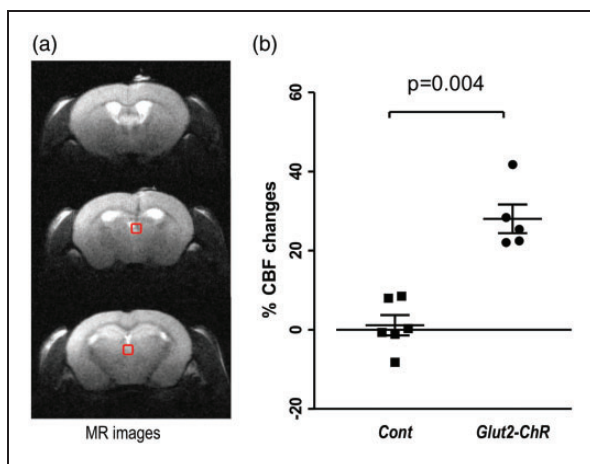


**Figure 6.** Optogenetic activation of *Glut2* neurons of the PVT increases local CBF. *Glut2* neurons of the PVT expressing channelrhodopsin were stimulated by light during CBF measurements. In anatomical MR images (a), squares indicate the location of the PVT. (b) Light-induced CBF increase in mice expressing channelrhodopsin (*Glut2-ChR*) in *Glut2* cells ( $n = 5$ ) but not in control mice (*Cont*) not expressing channelrhodopsin ( $n = 6$ ). Error bars were SEMs. Student unpaired *t*-test *p* value was 0.004.

areas, other hypoglycemia detection mechanisms may operate in the cortex.

Our optogenetics experiments showed that activation of channelrhodopsin-expressing *Glut2*-neurons of the PVT led to a robust increase in local CBF, similar in magnitude to that obtained following insulin-induced hypoglycemia. These PVT *Glut2* neurons have previously been described to control motivated feeding behavior through their projection to the nucleus accumbens,<sup>15</sup> a response that is activated by hypoglycemia or by *Glut2* inactivation. Whether the same neurons control feeding behavior and CBF is not known. From our present experiments, we do not know if activation of PVT *Glut2* neurons increase CBF also in the nucleus accumbens where their projections form a very dense network. Nevertheless, the fact that these PVT *Glut2* neurons are glutamatergic suggests that they control CBF through the release of glutamate, which has been reported to be a key signal to trigger the production of various vasodilators by astrocytes and neurons.<sup>1</sup>

The observation that in the absence of *Glut2*, the basal state CBF is high and not further increased by hypoglycemia is analogous to our previous report that plasma glucagon levels during euglycemic clamps are higher in *ripglut1;glut2<sup>-/-</sup>* mice than in control mice and are not further increased by hypoglycemia.<sup>39</sup> This, therefore, suggests that in the absence of *Glut2*, the hypoglycemia-sensing cells that normally express this transporter can no longer take up glucose, thereby causing an intracellular state of hypoglycemia, which

maintains the cells in an active state. The consequences are hyperglucagonemia and higher CBF in basal glycemic conditions. This also indicates that absence of *Glut2* from these sensing cells is not compensated by expression of another glucose transporter. In a previous study,<sup>19</sup> we also showed hypoglycemia-induced glucagon secretion could be restored in *ripglut1;glut2<sup>-/-</sup>* mice by transgenic expression of *Glut2* in astrocytes but not neurons. Here, we show that, at least in the PVT, *Glut2*-neurons can directly control CBF when activated by optogenetics. Whether CBF and glucagon responses depend on *Glut2* expression by different cell types, neurons vs. astrocytes, or whether hypoglycemia sensing in different brain regions rely on different cellular mechanisms that similarly control CBF and glucagon secretion is not known. However, our studies of *Glut2* neurons of the PVT<sup>15</sup> and the NTS<sup>14</sup> showed that, although they are both activated by hypoglycemia, the PVT neurons are glutamatergic and the NTS ones are GABAergic. Thus, there is probably a multiplicity of hypoglycemia sensing modalities, which control various physiological functions. These could be investigated using optogenetic approaches as used here to selectively activate the *Glut2* neurons of the PVT.

Collectively, our data show that *Glut2* expression by brain cells is required for the control CBF in response to variations in glucose concentrations. These cells could be neurons, as shown for the PVT *Glut2* neurons activated by optogenetics. But they could also be astrocytes, as these cells have been shown to also be involved in *Glut2*-dependent counterregulation.<sup>19</sup> One interesting aspect of these findings is that *Glut2* cells are present in most brain areas as dispersed cells with, however, a distinctly low abundance in the cortex, where sparse nerve terminals have been observed.<sup>17</sup> These *Glut2*-expressing cells may, therefore, form a global monitoring system that detect falls in glycemia and trigger area-specific increases in blood flow. More work is required to fully understand how activation of these cells increases CBF. However, as *Glut2* PVT neurons are glutamatergic and glutamate plays a critical role in controlling vasodilation,<sup>1</sup> glutamate release may be a key mediator of increased CBF. Our mouse models may be used to further dissect the link between hypoglycemia detection and increased CBF.

## Funding

The author(s) disclosed receipt of the following financial support for the research, authorship, and/or publication of this article: This work was supported by the Centre d'Imagerie BioMédicale (CIBM) of the University of Lausanne (UNIL), University of Geneva (UNIGE), Hôpitaux Universitaires de Genève (HUG), Centre Hospitalier Universtaire Vaudois (CHUV), and Ecole Polytechnique Fédérale de Lausanne (EPFL); and the Leenaards and

Jeantet Foundations. The work in BT's laboratory was supported by grants from the Swiss National Science Foundation (3100A0B-128657) and European Research Council Advanced Grant (INSIGHT and INTEGRATE).

### Declaration of conflicting interests

The author(s) declared no potential conflicts of interest with respect to the research, authorship, and/or publication of this article.


### Authors' contributions

Study concept and design: HL, RG and BT; acquisition of data: HL, FP, GL; analysis and interpretation of data: HL, FP, GL, RG, BT; drafting of the manuscript: HL, FP, GL, RG, BT. HL and BT are the guarantors of this work, had full access to all the data in the study and take responsibility for the integrity of the data and the accuracy of the data analysis.

### Supplementary material

Supplementary material for this paper can be found at the journal website: <http://journals.sagepub.com/home/jcb>

### ORCID iD

Hongxia Lei  <http://orcid.org/0000-0002-4065-9331>.

### References

- Attwell D, Buchan AM, Charpak S, et al. Glial and neuronal control of brain blood flow. *Nature* 2010; 468: 232–243.
- Belanger M, Allaman I and Magistretti PJ. Brain energy metabolism: focus on astrocyte-neuron metabolic cooperation. *Cell Metab* 2011; 14: 724–738.
- Verberne AJ, Sabetghadam A and Korim WS. Neural pathways that control the glucose counterregulatory response. *Front Neurosci* 2014; 8: 38.
- Bryan RM Jr and Pelligrino DA. Cerebral blood flow during chronic hypoglycemia in the rat. *Brain Res* 1988; 475: 397–400.
- Thomas M, Sherwin RS, Murphy J, et al. Importance of cerebral blood flow to the recognition of and physiological responses to hypoglycemia. *Diabetes* 1997; 46: 829–833.
- Teves D, Videen TO, Cryer PE, et al. Activation of human medial prefrontal cortex during autonomic responses to hypoglycemia. *Proc Natl Acad Sci U S A* 2004; 101: 6217–6221.
- Hoffman RG, Speelman DJ, Hinnen DA, et al. Changes in cortical functioning with acute hypoglycemia and hyperglycemia in type I diabetes. *Diab Care* 1989; 12: 193–197.
- Mangia S, Tesfaye N, De Martino F, et al. Hypoglycemia-induced increases in thalamic cerebral blood flow are blunted in subjects with type 1 diabetes and hypoglycemia unawareness. *J Cereb Blood Flow Metab* 2012; 32: 2084–2090.
- Horinaka N, Artz N, Jehle J, et al. Examination of potential mechanisms in the enhancement of cerebral blood flow by hypoglycemia and pharmacological doses of deoxyglucose. *J Cereb Blood Flow Metab* 1997; 17: 54–63.
- Burdakov D, Luckman SM and Verkhatsky A. Glucose-sensing neurons of the hypothalamus. *Phil Trans R Soc B* 2005; 360: 2227–2235.
- Routh VH. Glucose sensing neurons in the ventromedial hypothalamus. *Sensors* 2010; 10: 9002–9025.
- Marty N, Dallaporta M and Thorens B. Brain glucose sensing, counterregulation, and energy homeostasis. *Physiology* 2007; 22: 241–251.
- Steinbusch L, Labouebe G and Thorens B. Brain glucose sensing in homeostatic and hedonic regulation. *Trends Endocrinol Metabol* 2015; 26: 455–466.
- Lamy CM, Sanno H, Labouebe G, et al. Hypoglycemia-activated GLUT2 neurons of the nucleus tractus solitarius stimulate vagal activity and glucagon secretion. *Cell Metab* 2014; 19: 527–538.
- Labouebe G, Boutrel B, Tarussio D, et al. Glucose-responsive neurons of the paraventricular thalamus control sucrose-seeking behavior. *Nat Neurosci* 2016; 19: 999–1002.
- Arлуison M, Quignon M, Thorens B, et al. Immunocytochemical localization of the glucose transporter 2 (GLUT2) in the adult rat brain. II. Electron microscopic study. *J Chem Neuroanat* 2004; 28: 137–146.
- Arлуison M, Quignon M, Nguyen P, et al. Distribution and anatomical localization of the glucose transporter 2 (GLUT2) in the adult rat brain – an immunohistochemical study. *J Chem Neuroanat* 2004; 28: 117–136.
- Mounien L, Marty N, Tarussio D, et al. Glut2-dependent glucose-sensing controls thermoregulation by enhancing the leptin sensitivity of NPY and POMC neurons. *FASEB J* 2010; 24: 1747–1758.
- Marty N, Dallaporta M, Foretz M, et al. Regulation of glucagon secretion by glucose transporter type 2 (glut2) and astrocyte-dependent glucose sensors. *J Clin Invest* 2005; 115: 3545–3553.
- Thorens B. GLUT2, glucose sensing and glucose homeostasis. *Diabetologia* 2015; 58: 221–232.
- Williams DS, Detre JA, Leigh JS, et al. Magnetic resonance imaging of perfusion using spin inversion of arterial water. *Proc Natl Acad Sci U S A* 1992; 89: 212–216.
- Zhang W, Silva AC, Williams DS, et al. NMR measurement of perfusion using arterial spin labeling without saturation of macromolecular spins. *Magn Reson Med* 1995; 33: 370–376.
- Poulsen PH, Smith DF, Ostergaard L, et al. *In vivo* estimation of cerebral blood flow, oxygen consumption and glucose metabolism in the pig by [<sup>15</sup>O]water injection, [<sup>15</sup>O]oxygen inhalation and dual injections of [<sup>18</sup>F]fluorodeoxyglucose. *J Neurosci Methods* 1997; 77: 199–209.
- Videbeck P. PET measurements of brain glucose metabolism and blood flow in major depressive disorder: a critical review. *Acta Psychiatr Scand* 2000; 101: 11–20.
- Willats L, Connelly A and Calamante F. Improved deconvolution of perfusion MRI data in the presence of bolus delay and dispersion. *Magn Reson Med* 2006; 56: 146–156.
- Lei H, Pilloud Y, Magill AW, et al. Continuous arterial spin labeling of mouse cerebral blood flow using an

- actively-detuned two-coil system at 9.4T. *Conf Proc IEEE Eng Med Biol Soc* 2011; 2011: 6993–6996.
27. Muir ER, Shen Q and Duong TQ. Cerebral blood flow MRI in mice using the cardiac-spin-labeling technique. *Magn Reson Med* 2008; 60: 744–7448.
  28. Choi IY, Lee SP, Kim SG, et al. In vivo measurements of brain glucose transport using the reversible Michaelis-Menten model and simultaneous measurements of cerebral blood flow changes during hypoglycemia. *J Cerebr Blood Flow Metab* 2001; 21: 653–663.
  29. Thorens B, Guillam MT, Beermann F, et al. Transgenic reexpression of GLUT1 or GLUT2 in pancreatic beta cells rescues GLUT2-null mice from early death and restores normal glucose-stimulated insulin secretion. *J Biol Chem* 2000; 275: 23751–23758.
  30. Tarussio D, Metref S, Seyer P, et al. Nervous glucose sensing regulates postnatal beta cell proliferation and glucose homeostasis. *J Clin Invest* 2014; 124: 413–424.
  31. Cipolla MJ. *The cerebral circulation*. San Rafael (CA): Morgan & Claypool Life Sciences, 2009.
  32. Lei H, Poitry-Yamate C, Preitner F, et al. Neurochemical profile of the mouse hypothalamus using *in vivo*  $^1\text{H}$  MRS at 14.1T. *NMR Biomed* 2010; 23: 578–583.
  33. Speck O, Chang L, DeSilva NM, et al. Perfusion MRI of the human brain with dynamic susceptibility contrast: gradient-echo versus spin-echo techniques. *J Magn Reson Imaging* 2000; 12: 381–387.
  34. Gruetter R and Tkac I. Field mapping without reference scan using asymmetric echo-planar techniques. *Magn Reson Med* 2000; 43: 319–323.
  35. Constantinides C, Mean R and Janssen BJ. Effects of isoflurane anesthesia on the cardiovascular function of the C57BL/6 mouse. *ILAR J* 2011; 52: e21–e31.
  36. Bischof MG, Brehm A, Bernroider E, et al. Cerebral glutamate metabolism during hypoglycaemia in healthy and type 1 diabetic humans. *Eur J Clin Invest* 2006; 36: 164–169.
  37. Wang WT, Lee P, Yeh HW, et al. Effects of acute and chronic hyperglycemia on the neurochemical profiles in the rat brain with streptozotocin-induced diabetes detected using *in vivo*  $^1\text{H}$  MR spectroscopy at 9.4 T. *J Neurochem* 2012; 121: 407–417.
  38. Bady I, Marty N, Dallaporta M, et al. Evidence from glut2-null mice that glucose is a critical physiological regulator of feeding. *Diabetes* 2006; 55: 988–995.
  39. Burcelin R and Thorens B. Evidence that extrapancreatic GLUT2-dependent glucose sensors control glucagon secretion. *Diabetes* 2001; 50: 1282–1289.
  40. Dwyer KJ and Pardridge WM. Developmental modulation of blood-brain barrier and choroid plexus GLUT1 glucose transporter messenger ribonucleic acid and immunoreactive protein in rabbits. *Endocrinology* 1993; 132: 558–565.
  41. Hendrich KS, Kochanek PM, Melick JA, et al. Cerebral perfusion during anesthesia with fentanyl, isoflurane, or pentobarbital in normal rats studied by arterial spin-labeled MRI. *Magn Reson Med* 2001; 46: 202–206.
  42. Todd MM and Weeks J. Comparative effects of propofol, pentobarbital, and isoflurane on cerebral blood flow and blood volume. *J Neurosurg Anesthesiol* 1996; 8: 296–303.
  43. Schlünzen L, Cold GE, Rasmussen M, et al. Effects of dose-dependent levels of isoflurane on cerebral blood flow in healthy subjects studied using positron emission tomography. *Acta Anaesthesiol Scand* 2006; 50: 306–312.
  44. Duckrow RB, Beard DC and Brennan RW. Regional cerebral blood flow decreases during chronic and acute hyperglycemia. *Stroke* 1987; 18: 52–58.
  45. Duckrow RB. Decreased cerebral blood flow during acute hyperglycemia. *Brain Res* 1995; 703: 145–150.
  46. Wang Z, Luo W, Li P, et al. Acute hyperglycemia compromises cerebral blood flow following cortical spreading depression in rats monitored by laser speckle imaging. *J Biomed Opt* 2008; 13: 064023.
  47. Schwarzkopf TM, Horn T, Lang D, et al. Blood gases and energy metabolites in mouse blood before and after cerebral ischemia: the effects of anesthetics. *Exp Biol Med* 2013; 238: 84–89.
  48. Mujsce DJ, Christensen MA and Vannucci RC. Regional cerebral blood flow and glucose utilization during hypoglycemia in newborn dogs. *Am J Physiol* 1989; 256: H1659–H1666.
  49. Auer RN. Hypoglycemic brain damage. *Metab Brain Dis* 2004; 19: 169–175.
  50. Abdelmalik PA, Shannon P, Yiu A, et al. Hypoglycemic seizures during transient hypoglycemia exacerbate hippocampal dysfunction. *Neurobiol Dis* 2007; 26: 646–660.